Nephrol Dial Transplant (2011) 26: 3930–3937
doi: 10.1093/ndt/gfr131
Advance Access publication 31 March 2011

Gammopathy with IgA mesangial deposition provides a monoclonal model of IgA nephritogenicity and offers new insights into its molecular mechanisms

Ahmed Boumediene[1,2,*], Christelle Oblet[1,2,*], Zeliha Oruc[1,2], Sophie Duchez[1,2], Willy Morelle[3], Anne Huynh[4], Jacques Pourrat[4], Jean-Claude Aldigier[1,2†] and Michel Cogné[1,2†]

[1]Laboratoire d'Immunologie et Service de Néphrologie, Hôpital Universitaire Dupuytren, Université de Limoges, Limoges, France, [2]CNRS, UMR 6101, Limoges, France, [3]Glycobiologie Structurale et Fonctionnelle, Unité Mixte de Recherche CNRS/USTL 8576, IFR 147, Bâtiment C9, Université des Sciences et Technologies de Lille 1, Villeneuve d'Ascq Cedex, France and [4]Service d'Hématologie et Service de Néphrologie et d'Immunologie clinique, Hôpital Purpan, Toulouse, France

Correspondence and offprint requests to: Michel Cogné; E-mail: michel.cogne@unilim.fr
*These authors equally contributed to the experimental part of this work.
†These authors equally contributed to this work as senior authors.

Abstract

Background. Henoch–Schönlein purpura (HSP) and IgA nephropathy (IgAN) are characterized by mesangial deposition of polyclonal IgA eventually showing aberrant glycosylation, affinity for mesangial cells and/or co-precipitation with antigen, bacterial peptides, autoantibodies or soluble receptors. IgA were also suggested to be negatively charged and predominantly of λ type but rarely in a monoclonal form.

Methods. A gammopathy case with HSP provided us with a unique molecularly defined nephritogenic IgA1λ. Immunological analysis, biological activities, glycosylation analysis and finally IgA sequence were determined.

Results. Compared to IgA1 from healthy subjects or IgAN patients, IgA1 CAT showed hyposialylation but no hypogalactosylation, in agreement with underexpression of sialyltransferase genes by the plasma cell clone. IgA variable domains had low pIs with negatively charged complementarity-determining regions. Weak reactivity appeared against the cationic autoantigen lactoferrin, which was, however, absent from kidney deposits. Deposition also occurred in mice upon injection of only the polymeric form of IgA1 CAT, despite whether or not co-injected with lactoferrin.

Conclusions. This monoclonal model of IgA nephritogenicity strongly suggests that beside hinge region glycosylation, V domains play a role in IgA stability and pathogenicity and supports the hypothesis that responses against cationic epitopes from pathogens or autoantigens may select negatively charged complementarity-determining regions prone either to bind charged structures of the mesangium or to promote by themselves IgA aggregation and deposition.

Keywords: Henoch–Schönlein purpura; IgA-ANCA; IgA monoclonal gammopathy; necrotizing vasculitis

Introduction

Henoch–Schönlein purpura (HSP) is a form of vasculitis in which multiple tissues are affected with IgA deposition, while IgA nephropathy (IgAN) is restricted to kidney mesangium deposits. Deposited IgA, usually polyclonal, may show antigen co-precipitation, low charge or aberrant galactosylation of the hinge region, correlating with the occurrence of autoantibodies against hypogalactosylated IgA [1–3]. However, these abnormalities are neither constant nor specific. Interestingly, deposits of murine IgA can occur despite absence of an *O*-glycosylated hinge [4, 5]. Beside glycosylation, other IgA characteristics deserve exploration.

The rare association of IgA gammopathy with HSP or IgAN [6–10] (Table 1) has never been explored in detail, despite the unique interest of pathogenic IgAs with defined structures. For such a molecule, we determined sequence, glycosylation, antigen specificity and binding to kidney. This first complete description of a nephritogenic IgA gives insight into the process of mesangial deposition and provides a new pathophysiological model.

Materials and methods

IgAN patients and control individuals

Patients and controls gave their informed consent, and the study was approved by the local ethical committee.

A 66-year-old woman (patient CAT) suffering from vasculitis was admitted in the nephrology unit after the discovery of nephrotic syndrome with microscopic haematuria and worsening renal function.

Five years earlier, a palpable purpuric rash located on legs and abdomen had appeared along with arthralgias. Clinical examination did not show any other distinctive characteristics. Extensive explorations were performed; no cryoglobulinaemia was found and a monoclonal IgA was discovered (IgA: 330 mg/dL, IgG: 203 mg/dL and IgM: 40 mg/dL);

Table 1. Molecular features of IgA molecules in the six reports of IgA deposition potentially involving a monoclonal IgA component; ND, not determined

Report	M component	ANCA activity	Decreased hinge hyposialylation	Decreased hinge galactosylation
Dosa *et al.* [11]	IgAκ	ND	ND	ND
Birchmore *et al.* [7]	IgAκ	−	ND	ND
Zickerman *et al.* [10]	IgA1	+ (proteinase 3)	Yes	No
Van der Helm *et al.* [9]	IgA1κ	−	Yes	No
Arrizagabala *et al.* [6]	IgA (monoclonal?)	−	ND	ND
This report	IgA1λ	+ (lactoferrin)	Yes	No

Table 2. Immunologic laboratory characteristics of the patient CAT; NR, normal range

Autoantibody	Results
Antinuclear antibody	Negative at 1/60 dilution
Anti-ds DNA	Negative
Anti-Ro (SSA) antibody	Negative
Anti-La (SSB) antibody	Negative
Anti-RNP antibody	Negative
Anticardiolipin IgM and IgG	Negative
Goodpasture's antibody	Negative
Cryoglobulins	Negative
ANCA	Present (1/1600 dilution) of IgA subtype
Total complement serum	563 mg/L NR (324–406)
C3 complement	750 mg/L NR (780–1510)
C4 complement	240 mg/L NR (170–540)
Hepatitis B antigen	Negative
Hepatitis C antibody	Negative
IgG	169 mg/dL
IgA	272 mg/dL
IgM	28 mg/dL

however, no laboratory findings supported the diagnosis of myeloma. Four years earlier, gastrointestinal symptoms, such as abdominal pain occurred. Over those 5 years, she received prednisone at different doses and plasmapheresis for vasculitis. Six months before admission, thalidomide treatment was proposed because of the increased frequency of vasculitis outbreaks; this treatment was stopped after 2 months because of electromyographic anomalies.

The patient was then referred to the nephrology unit because of renal involvement. She had no family history of renal disease or autoimmune disorders. She had no known allergies; she knew of no exposures to toxins.

On examination, she appeared chronically ill. Her blood pressure was 170/90 mmHg; palpable purpuric lesions were present on the patient's feet and abdomen. The rest of the physical examination was normal. Serum creatinine level was 1.7 mg/dL (150 µmol/L) and urinalysis revealed 10–15 red cells per high-power field and a 24-h urine collection showed 4 g of proteinuria. Other blood chemical values were haematocrit 35%, albumin 23 g /dL, alkaline phosphatase 98 U/L, aspartate aminotransferase 48 U/L. Some immunologic values of the patient are summarized in Table 2.

A skin biopsy specimen showed leucocytoclastic vasculitis. Direct immunofluorescence staining of the biopsy showed granular deposits of IgA of the λ subtype in a vascular pattern (Figure 1A).

Renal biopsy was performed and the diagnosis of focal segmental necrotizing glomerulonephritis was made (Figure 1B); diffuse mesangial IgA deposits were observed with only λ type light chain together with C3 and fibrin; immunofluorescence was negative with anti-µ, -γ and -κ immunoglobulins chains; no vascular staining was observed (Figure 1C and D).

Again, there was no support for myeloma including bone marrow aspiration (7% plasmocytes) and biopsy. Treatment with oral prednisone and cyclophosphamide administered intravenously (IV) was started. The patient received over the course of 1 year, 11 perfusions of cyclophosphamide [(750 mg/m2 of body surface area (BSA)]. This treatment finally became ineffective and the patient underwent weight loss, polyarthritis, purpura, proteinuria (3.5 g/day) and rapidly progressive kidney failure (creatininémia: 3.4 mg/dL), while IgA and Anti-Neutrophil Cytoplasmic antibody (ANCA) levels increased (IgA: 438 mg/dL, IgG: 276 mg/dL and IgM: 50 mg/dL IgA-ANCA: >1600). This led to a switch in the therapeutic approach to high-dose melphalan (100mg/m2 BSA) and autograft with peripheral stem cells previously collected after mobilization with cyclophosphamide (2 g/m^2 SC) and Granulocyte-Colony Stimulating Factor. The result of this treatment was satisfactory; 3 months after the autograft, the patient was well; all clinical symptoms disappeared, the nephrotic syndrome was in complete remission, proteinuria disappeared and plasma creatinine was at 1.5 mg/dL (132 µmol/L) (IgA: 133 mg/dL, IgG: 369 mg/dL, IgM: 41 mg/dL and IgA-ANCA: 200 U).

The patient remained in a state of remission for one year; she received 20 mg prednisolone every other day; then, unfortunately, symptoms such as purpura, polyarthritis and digestive tract manifestations gradually reappeared more and more frequently. IgA level was 400 mg/dL and IgA-ANCA: >1200 U). A vasculitis treatment was started again with oral corticosteroids and cyclophosphamide.

Two years later, the patient is well, her vasculitis outbreaks are few and far between; the treatment regimen consists of low-dose corticosteroids and low-dose cyclophosphamide. (IgA: 78 mg/dL, IgG: 369 mg/dL, IgM: 41 mg/dL and IgA-ANCA: 200 U).

IgA purification

IgA1 was purified by chromatography using jacalin affinity (Pierce, Rockford, IL). Monomeric IgA1 (mIgA1) and polymeric IgA1 (pIgA1) were separated by size exclusion chromatography using HiPrep 16/60 Sephacryl S-200 HR prepacked column, XK 26/100 column and XK 16/70 column filled with Sephacryl S-200 HR resin and with Superdex 200 prep grade resin (GE Healthcare, Waukesha, WI), respectively.

Immunoassays and lectin-binding assays

Autoantibodies against the cytoplasm of polynuclear cells (ANCA) of the IgG and IgA classes were assayed by immunofluorescence on human neutrophils. Further analysis of specificity was done by enzyme-linked immunosorbent assay (ELISA) following the instructions of the manufacturer (ANCA Profile ELISA; Euroimmun) against the six most classical ANCA targets myeloperoxydase, proteinase 3, cathepsin G, neutrophil elastase, bactericidal/permeability-increasing protein and lactoferrin. Inhibition of lactoferrin binding was evaluated by incubating the patient serum with an excess of soluble lactoferrin (5 mg/mL) for 1 h at 37°C prior to the immunofluorescence assay on human neutrophils. IgA-class rheumatoid activity was assayed by ELISA as described [12].

Purified IgA1 was analysed by western blot using horseradish peroxidase (HRP)-linked goat anti-human IgA antibodies (Beckman Coulter, Fullerton, CA). Human J chain and human secretory component were detected using rabbit anti-human J chain and rabbit anti-human secretory component (a kind gift of Dr. Blaise Corthesy, Lausanne), followed by incubation with HRP-linked goat anti-rabbit antibody (Bio-Rad, Hercules, CA). After washing, the signal was measured by chemiluminescence (ECL plus; GE Healthcare, Waukesha, WI).

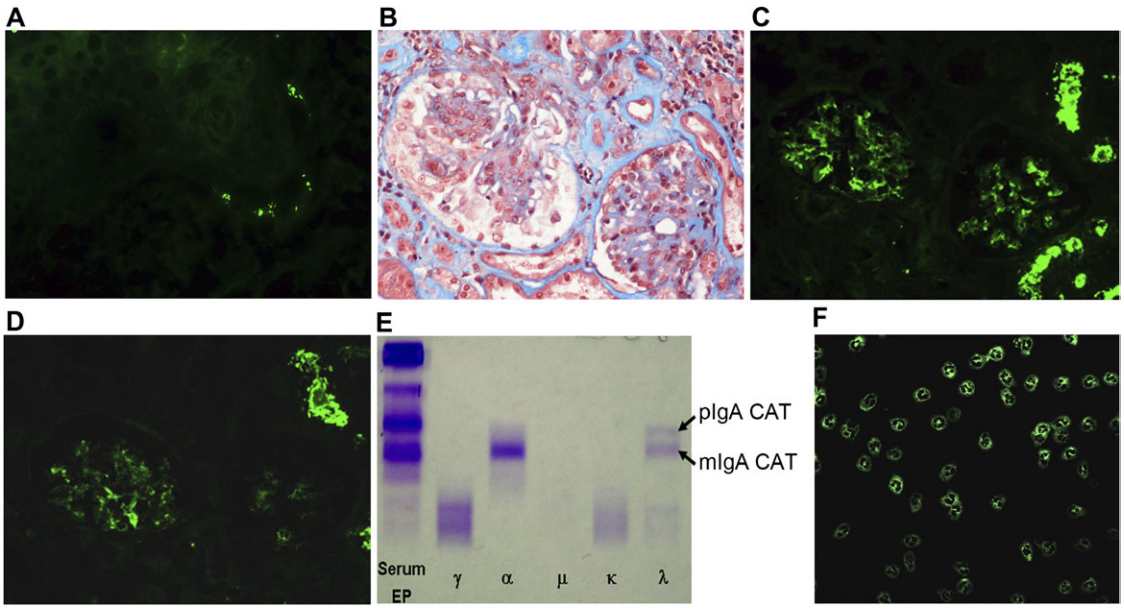

Fig. 1. Pathological and immunological findings in patient CAT. (**A**) Skin biopsy of patient CAT showing IgA deposits in superficial dermis vessels. (**B**) Kidney sections of patient CAT observed by light microscopy (Hematein eosine, 400×). (**C**) and (**D**) Consecutive slices of patient CAT kidney biopsy stained with fluorescent anti-α Ig heavy chain or anti-λ Ig light chain antisera, respectively. (**E**) Patient CAT analysis by serum electrophoresis (serum EP) and immunofixation with specific antisera to γ, α, and μ heavy chains or κ and λ light chains. The monoclonal component migrates as a double band indicated by arrows. (**F**) ANCA activity of IgA CAT. Patient CAT serum or purified IgA shows a cytoplasmic pattern when incubated on ethanol-fixed cytospins of human neutrophils and revealed with a secondary fluorescent anti-IgA conjugate.

For lectin assays, purified IgA1 were diluted in 0.2% gelatin, added to wells and incubated for 2 h at 37°C. After washing, wells were incubated with biotinylated lectins, revealed with Avidin–HRP conjugate (Sigma-Aldrich). Bound IgA1 were detected using polyclonal goat anti-human IgA antibody conjugated with HRP (Beckman Coulter). Revelation was with *o*-phenylenediamine.

The results of lectin assays are expressed as mean ± SEM. Binding of IgA1 from IgAN patients and control group were compared using two-tailed Student's *t*-test. Differences were considered statistically significant at $P < 0.05$.

In vivo experiments

Nude mice (12–14 weeks old) were injected intravenously with 400 μg of human mIgA1 or pIgA1. CAT IgA1 was injected with or without a 2-fold molar excess of the lactoferrin antigen. Purified IgA1 of healthy individuals was used as control. Animals were sacrificed after 2 h. Frozen kidney sections (6 μm thick) were fixed in acetone and examined by immunofluorescence for deposits using fluorescein-labelled goat $F(ab')_2$ anti-human IgA (Southern Biotechnology).

C57/BL6 mice (8 weeks old) were injected intravenously with sera from a healthy control (11 mice) or patient CAT (11 mice) in volumes corresponding to 700 μg of total IgA in both cases. Animals were sacrificed after 2 h and immunofluorescence was performed as described above.

Release, preparation and mass spectrometry analysis of glycans

Purified IgA1 was reduced and carboxyamidomethylated, followed by sequential tryptic and peptide *N*-glycosidase F-digestion and Sep-Pak® purification (Waters, Milford, MA). Putative *O*-glycopeptides remaining after PNGase F-digestion of the tryptic glycopeptides were subjected to reductive elimination. Permethylation of the freeze-dried glycans, sample clean-up and maldi assisted laser desorption/ionisation- time of flight-mass spectrometry was analysed.

Plasmocytes sorting and real-time polymerase chain reaction

CAT bone marrow plasma cells were purified after labelling by a PE-conjugated anti-CD138 antibody (Immunotech, Marseille, France), using anti-PE-coupled magnetic beads and MACS separation (Miltenyi Biotec, Bergisch Gladbach, Germany). Cell purity as assessed by flow cytometry was >98%.

Polymerase chain reactions (PCRs) were carried out in Micro Fluidic Cards using the ABI PRISM 7900HT Sequence Detection System (Applied Biosystems, Foster City, CA) according to the manufacturer's instructions. Data were analysed using the threshold cycle (C_t) relative quantification method. C_t values ranged from 0 to 40 (the latter represents the default upper limit PCR cycle number defining failure to detect a signal). Genes with no or very low signal ($C_t > 35$) in most samples were eliminated. The relative amount of each transcript was normalized to 18S transcript in the same cDNA to obtain the $\triangle C_t$. A $\triangle\triangle C_t$ was then obtained to calculate the comparative gene expression between a calibrator sample (in this case, polyclonal CD138+ plasma cells sorted from normal human bone marrow) and the other samples. The formula $2^{-\triangle\triangle C_t}$ was applied to calculate the relative expression of target genes.

PCR cloning and IgA sequencing

Total RNA was extracted from the patient's bone marrow and 1 μg was reverse transcribed for 1 h with Superscript® (Life Technologies, Carlsbad, CA). The clonally rearranged VDJ of the patient IgA heavy chain was repetitively amplified using six different 5′ primers corresponding to consensus sequences of variable V_H subgroup leader regions and 3′ primers complementary to human Cα exons CH1, CH2 and CH3: V_H1 5′-CCATGGACTGGACCTGGA-3′;x V_H2 5′-ATGGACATACTTTGTTCCAC-3′; V_H3 5′-ATGGAGTTTGGGCTGAGCT-3′; V_H4 5′-ATGAAACACCTGTGGTTCTTCCTCCT-3′; V_H5 5′-ATGGGGTCAACCGCCATCC-3′; V_H6 5′-ATGTCTGTCGTCTCCTTCCTCAT-3′; CH1α 5′-TGAGTGGCTCCTGGGGAAGAA-3′ CH2α 5′-TCGGGGTGGCAGCATGAGG-3′ and CH3α 5′-ACAGGCGGGCGGCTCAGTA-3′

For the λ chain, PCR primers were a 5′ primer corresponding to a Vλ1-Vλ2-Vλ3 consensus leader region (5′-ATGGCCKGSWYYSYTCTCCTC-3′) and a 3′ primer complementary to the consensus upstream part of the Cλ exons (5′-CTCCCGGGTAGAAGTCACT-3′).

Results

Pathological and immunological findings in patient CAT

Patient CAT analysis by serum electrophoresis (serum EP) and immunofixation with specific antisera to γ, α, μ heavy chains or κ, λ light chains show a monoclonal λIgA pattern (Figure 1 C–E). The search for an IgA-class rheumatoid

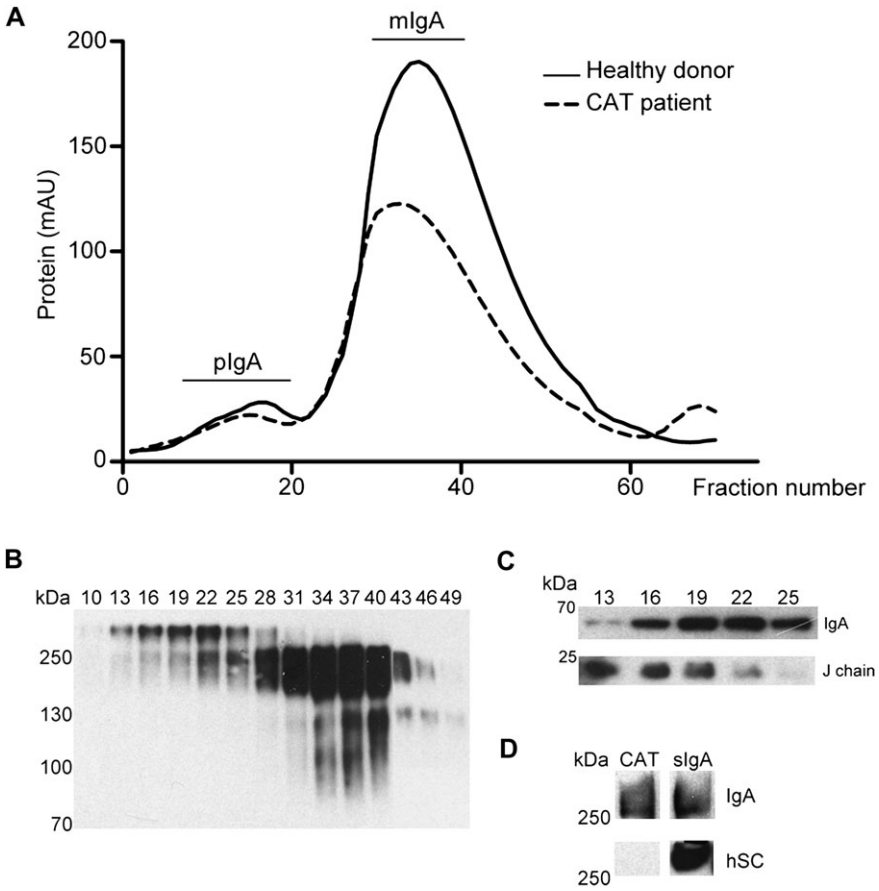

Fig. 2. Molecular structure of the serum IgA1. (**A**) Elution profile of mIgA1 and pIgA1 from patient CAT and from a healthy donor. Absorbance values were read at 280 nm. Eluted fractions are indicated and were further studied by western blots. (**B**) Analysis of representative fractions after 6% sodium dodecyl sulphate–polyacrylamide gel electrophoresis (PAGE-SDS) under non-reducing conditions. The various molecular forms of IgA1 CAT were detected using anti-human IgA antibody. (**C**) Detection of the presence of J chain in representative fractions after 12% PAGE-SDS under reducing conditions. (**D**) Western blot analysis showing the absence of secretory component in unfractionated IgA1 CAT after 6% PAGE-SDS under non-reducing conditions. IgA1 CAT was compared to purified secretory IgA used as a positive control. The signal was detected using an anti-human secretory component antiserum.

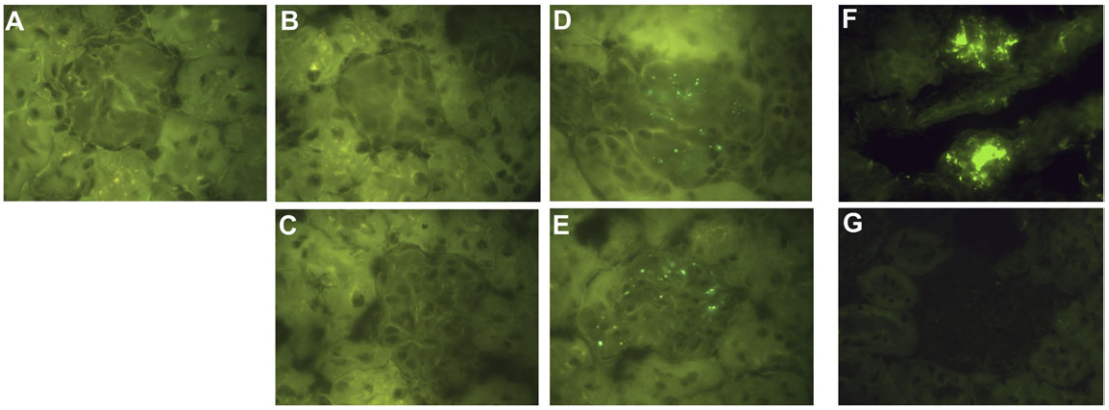

Fig. 3. Search for *in vivo* deposited IgA 2 h after IV injection of IgA into mice (**A –E**: nude mice; **F** and **G:** C57/BL6 mice). Injections were carried out with IgA from various origins (**A –E**: purified IgA1; **F** and **G**: complete serum). (**A**) FPLC purified pIgA from a healthy control. (**B**) FPLC -purified mIgA1 from patient CAT. (**C**) FPLC -purified mIgA1 from patient CAT, co-injected with its cognate antigen lactoferrin. (**D**) FPLC -purified pIgA1 from patient CAT. (**E**) FPLC -purified pIgA1 from patient CAT, co-injected with its cognate antigen lactoferrin. (**F**) IgA deposition in normal mice injected with serum from patient CAT. (**G**) Absence of any IgA deposits in normal mice injected with normal human serum.

factor proved negative (data not shown). IgA-class ANCA proved clearly positive by immunofluorescence on human and mouse neutrophils with a cytoplasmic pattern (Figure 1F) and typed by ELISA as negative against myeloperoxydase, proteinase 3, cathepsin G, bactericidal/permeability-increasing protein and neutrophil elastase. In contrast, this ELISA assay was scored as weakly positive against lactoferrin (value for the patient in the profile ANCA assay was

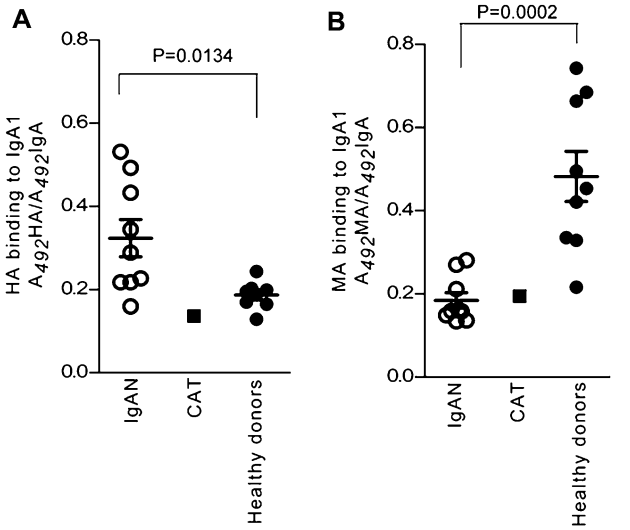

Fig. 4. Glycosylation analysis by lectin bindig assays. (**A**) *Helix aspersa* (HA) lectin binding of IgA1. CAT IgA1 did not show any binding difference to HA when compared to healthy donors ($n = 8$) in contrast to IgAN patients ($n = 9$) (P = 0.0134). (**B**) *Maackia amurensis* (MA) lectin binding of IgA1. Healthy donors IgA1 ($n = 9$) showed significantly higher MA binding (2.5-fold) than that of CAT IgA1 and IgA1 nephropathy controls ($n = 9$) (P = 0.0002). P-values were generated using two-tailed Student's *t* -test. CAT IgA1 (closed squares); healthy donors (closed circles); IgAN patients (open circles).

1.8, while negative results were indicated as follows 1.0, weakly positive assays as $\geq$1.0 and $\leq$2.0 and positive assays as $\geq$2.0). However, the c-ANCA-positive pattern could not be inhibited by pre-incubating the serum with an excess of soluble lactoferrin prior to the immunofluorescence assay. The various forms of IgA1 were purified from the serum of patient CAT and from control serum by affinity chromatography. As shown in chromatograms (Figure 2A), two retention peaks for both IgA1 CAT and control IgA1 were detected. IgA1 content was tested by anti-human IgA immunoblot (Figure 2B). IgA1 polymers were recovered in Peak 1, whereas monomers were in Peak 2.

Gel electrophoresis under reducing and non-reducing conditions was performed. Western blot analysis showed that CAT pIgA1 was associated with J chain but not with any S component (Figure 2C and D).

CAT IgA biological activities

Immunodeficient mice were injected with monomeric (mIgA1) or polymeric (pIgA1) IgA purified from patient CAT or from a healthy control: only CAT IgA1 under the form of pIgA1 yielded deposits, despite whether or not lactoferrin was co-injected. Two groups of 11 C57/BL6 mice injected with sera with equivalent amounts of IgA from CAT and control were analysed and only showed mesangial IgA deposits upon CAT serum injection (Fisher's exact test, P < 0.0001) (Figure 3).

IgA glycosylation

Helix aspersa-binding terminal *N*-acetylgalactosamine (GalNAc) similarly bound IgA1 CAT and IgA1 from healthy subjects (Figure 4A). Binding was higher to IgA1 from other IgAN patients (P = 0.0134) showing that only the latter was hypogalactosylated.

Maackia amurensis binding to sialic acids was higher for IgA1 from healthy donors than from IgAN patients or patient CAT (P = 0.0002), indicating hyposialylation of the latter (Figure 4B).

Table 3. Transcription analysis for a series of genes involved in glycosylation[a]

	Fold over/underexpression
Overexpressed genes in CAT plasma cells	
Chondroitin sulphate proteoglycan (versican)	↑ 850-fold
Collectin 10	↑ 14-fold
Galactose-3-*O*-sulphotransferase 2	↑ 13-fold
Underexpressed genes in CAT plasma cells:	
Beta 1,4-galactosyltransferases	
B4GALT5	↓ 43-fold
B4GALT6	↓ 1140-fold
Sialyltransferases	
SIA T4A	↓ 10-fold
SIA T4B	↓ 5-fold
SIA T4C	↓ 814-fold
SIA T7A	↓ 1431-fold
SIA T7B	↓ 1092-fold
SIA T7C	↓ 701-fold
SIA T8A	↓ 245-fold
Fucosyltransferase 1	↓ 1941-fold
Sulphotransferases	
CHST10	↓ 91-fold
CHST13	↓ 85-fold
CHST1	↓ 176-fold
Galectins	
LGALS12	↓ 2938-fold
LGALS2	↓ 154-fold
LGALS3BP	↓ 20-fold
LGALS4	↓ 200-fold
LGALS9	↓ 104-fold
Siglecs	
SIGLEC10	↓ 709-fold
SIGLEC11	↓ 352-fold
SIGLEC5	↓474-fold
SIGLEC6	↓ 347-fold
SIGLEC7	↓ 193-fold
SIGLEC9	↓ 118-fold
SIGLECL1	↓ 32-fold
Syndecans	
SDC2	↓ 1448-fold
SDC3	↓ 13-fold
SDC4	↓ 153-fold

[a]Expression in the CAT patient plasma cells was compared with expression in purified polyclonal plasma cells from a healthy control. Genes with the most important overexpression or underexpression in CAT plasma cells are shown.

Glycosylation analysis of IgA by mass spectrometry

MALDI-TOF-MS analysis compared CAT IgA1 *N*-glycans with purified IgA1 from a healthy control. The latter showed >90% predominance of biantennary sialylated oligosaccharides and increased abundance of the neutral biantennary glycan (m/z 2070). For *O*-glycans, three major ions were observed at m/z 534 (Hex1HexNAcitol), 895 (Neu5Ac1Hex1HexNAcitol) and 1256 (Neu5Ac2Hex1HexNAcitol) with an increase of the relative abundance of the neutral glycan Hex1HexNAcitol (m/z 534) in CAT IgA1, consistent with hyposialylated *O*-glycans (Supplementary figure S1).

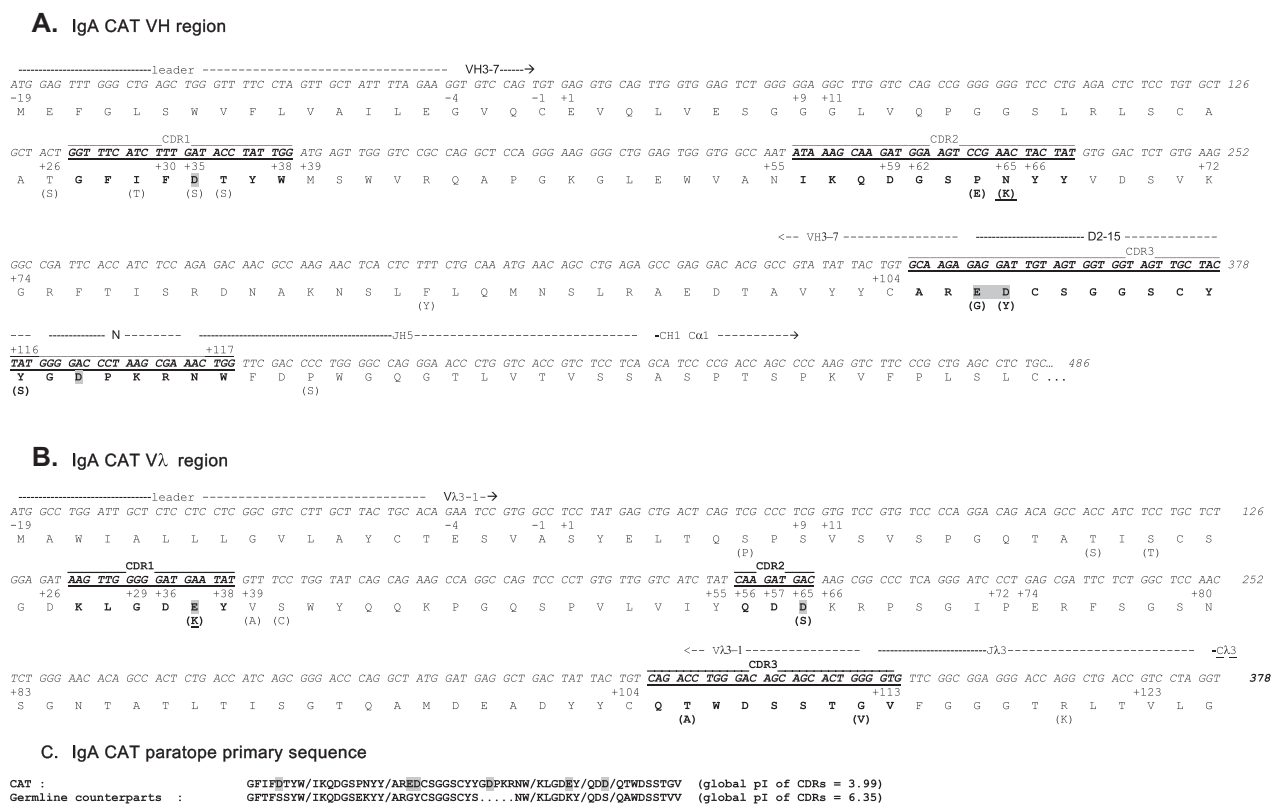

Fig. 5. Sequence analysis of IgA1 CAT. Nucleotide sequences show the junctions between V, D and J segments. The deduced protein sequences are provided immediately below and show the substitutions (residues normally present at these positions in the germline sequences indicated between parentheses). (**A**) Heavy chain variable domain. (**B**) Light chain variable domain. (**C**) Theoretical peptide combining the six VH and Vλ CDR regions of the IgA CAT antigen-binding site, compared to its germline counterpart.

Glycosyltransferase gene expression

CAT bone marrow plasma cells showed consistent variations in glycosyltransferases gene expression. The main IgA1 hinge O-linked glycans are (NeuAc a2,3Gal β1,3GalNAc), synthesized by β1,3-galactosyltransferase (C1GALT1 gene) transferring galactose onto *N*-acetylgalactosamine and α2,3-sialyltransferases (SIAT4 genes) transferring sialic acid onto Galβ1,3GalNAc.

All three α2,3-sialyltransferases (SIAT4A, 4B and 4C) were underexpressed in CAT cells, in agreement with the observed IgA1 under-sialylation. In contrast, C1GALT1 was barely altered. Interestingly, expression of β1,4-galactosyltransferase genes was decreased. Additional glycosylation or glycan receptors genes showed decreased expression, including galectins, siglecs and syndecan . . . (Table 3).

IgA sequence

IgA CAT structure was deduced from plasma cells cDNA. A normal Cα1 carried a VH3-7/D2-15/JH5 segment with 11 substitutions by comparison to germline. The Vλ3/Jλ3/Cλ3 λ chain showed 10 replacements. Altogether, five of the six complementarity-determining regions (CDR) showed replacements negatively charging them: VH-CDR1, Ser35 →Asp (acidic); VH-CDR2, Lys 65 (basic) → Asn (neutral); VH-CDR3, Gly107 → Glu (acidic), Tyr108 → Asp (acidic) and insertion of Asp(acidic) at position 116C in-between D and JH; Vλ-CDR1, Lys37 (basic) → Glu (acidic); Vλ-CDR2, Ser65 (neutral) → Asp (acidic). The λ chain carried substitutions of hydrophobic with neutral residues (Ala104 → Thr and Val112 → Gly). Calculated isoelectric points (pI) were, respectively, 5.08 and 4.09 for the VH and Vλ domains (instead of 7.88 and 4.54 for their germline counterparts).

Linking all six VH and Vλ CDRs for pI calculations gave 3.99 for the CAT CDRs (GFIFDTYWIKQDGSPNYYA-REDCSGGSCYYGDPKRNWKLGDEYQDDQTWDSST-GV) versus 6.35 for the assembled germline counterpart (GFTFSSYWIKQDGSEKYYARGYCSGGSCYSNWKL-GDKYQDSQAWDSSTVV) (Figure 5).

Discussion

IgA mesangial deposition remains a poorly understood process. Its occurrence during gammopathies might be underestimated in patients suffering severe direct complications of plasma cell malignancies. Only six reports, including ours, mentioned monoclonal mesangial IgA deposition (Table 1) [6, 7, 9–11]. Hinge hyposialylation but not hypogalactosylation was found in three cases. In our study, it was indicated by both lectin assays and mass spectrometry, and further confirmed by consistent variations of glycosyltransferases expression. Decreased expression of β1,4-galactosyltransferases (transferring galactose to both O- and N-linked saccharides) did not result in

biochemically measurable undergalactosylation, a discrepancy indicating that these enzymes are not rate limiting. They encode galactosyltransferases synthesizing *N*-glycans (thus uninvolved into hinge glycosylation) whose defect promoted IgA deposition in mice [13]. In previously reported IgAN cases in human, alterations of *N*-glycosylation have also been observed [14].

In the cases of gammopathies associated with IgA deposition, ANCA activity was only found twice, against lactoferrin (this report) and proteinase 3 [10] and appears inconstant for monoclonal IgA as well as polyclonal IgA in HSP and IgAN. In the case of CAT, the ELISA reactivity against lactoferrin was weak and the c-ANCA immunofluorescence pattern could not be inhibited by an excess of soluble lactoferrin, raising the hypothesis that ANCA activity might also be against another unidentified ANCA antigen-binding lactoferrin or showing cross-reactivity with lactoferrin. In the case of CAT, the same monoclonal immunoglobulin carries two nephritogenic activities with both a tendency to form deposits in the mesangium and an autoantibody ANCA activity responsible for vasculitis. These two properties are thus likely to both contribute to glomerular injury.

Both light chain types were reported in monoclonal IgA deposition cases (Table 1), while an increased λ/κ ratio was reported in deposited polyclonal IgA from IgAN [15, 16]. Besides being more acidic than pIgAκ, pIgAλ were shown to bind more frequently human mesangial cells [17]. Anionic IgA from IgAN also interacted more strongly with mesangial cells after preincubation with poly-L-lysine cations [1]. It remains to be determined whether endogenous cations might also promote deposition.

This study revealed strong acidic V domains in IgA1 CAT and demonstrated the ability of this immunoglobulin to yield glomerular deposits in mice, despite whether or not the lactoferrin antigen was co-injected. Since immunoglobulin variability focuses on CDRs, it is likely that the more acidic pIgA are those with acidic CDR. A tempting hypothesis is that responses to some cationic epitopes might select anionic CDRs, potentially decreasing pIgA stability and/or promoting binding to mesangium cationic structures. Of note, known targets of monoclonal or polyclonal pIgA in IgAN or HSP [18, 19] include cationic antigens such as lactoferrin (pI: 8.17), proteinase 3 (pI: 8.42) and gliadin (pI: 8.58). IgA from IgAN were also reported to preferentially bind cationic polypeptides [20]. However, since mutations affect both CDR and framework regions, it will be interesting to characterize a higher number of nephritogenic monoclonal IgA structures. This study recalls that one should be aware of the possibility of IgA deposition in the course of gammopathies. It also strongly suggests that IgA deposition does not only involve defective glycosylation favouring aggregation with antigens and/or anti-IgA IgG [3] but also strongly relies on the V region structure and the antigen-binding sites electrostatic charge.

Supplementary data

Supplementary data is available online at http://ndt.oxfordjournals.org

Acknowledgements. The authors would like to thank Dr. Anne Modesto-Segonds for histopathological studies of the patient's kidney and Dr. Renato Monteiro for critical reading of the manuscript.

This work was supported by grants from Agence Nationale de la Recherche, Ligue Nationale contre le Cancer and Conseil Régional du Limousin. The mass spectrometry facility used in this study was funded by the European Community (FEDER), the Région Nord-Pas de Calais (France) and the Université des Sciences et Technologies de Lille I.

Conflict of interest statement. None declared.

References

1. Leung JC, Tang SC, Lam MF *et al.* Charge-dependent binding of polymeric IgA1 to human mesangial cells in IgA nephropathy. *Kidney Int* 2001; 59: 277–285
2. Suzuki H, Moldoveanu Z, Hall S *et al.* IgA1-secreting cell lines from patients with IgA nephropathy produce aberrantly glycosylated IgA1. *J Clin Invest* 2008; 118: 629–639
3. Tomana M, Novak J, Julian BA *et al.* Circulating immune complexes in IgA nephropathy consist of IgA1 with galactose-deficient hinge region and antiglycan antibodies. *J Clin Invest* 1999; 104: 73–81
4. Imai H, Nakamoto Y, Asakura K *et al.* Spontaneous glomerular IgA deposition in ddY mice: an animal model of IgA nephritis. *Kidney Int* 1985; 27: 756–761
5. Launay P, Grossetete B, Arcos-Fajardo M *et al.* Fcalpha receptor (CD89) mediates the development of immunoglobulin A (IgA) nephropathy (Berger's disease). Evidence for pathogenic soluble receptor-Iga complexes in patients and CD89 transgenic mice. *J Exp Med* 2000; 191: 1999–2009
6. Arrizabalaga P, Saurina A, Sole M *et al.* Henoch-Schonlein IgA glomerulonephritis complicating myeloma kidneys: case report. *Ann Hematol* 2003; 82: 526–528
7. Birchmore D, Sweeney C, Choudhury D *et al.* IgA multiple myeloma presenting as Henoch-Schonlein purpura/polyarteritis nodosa overlap syndrome. *Arthritis Rheum* 1996; 39: 698–703
8. Preud'homme JL, Aucouturier P, Touchard G *et al.* Monoclonal immunoglobulin deposition disease (Randall type). Relationship with structural abnormalities of immunoglobulin chains. *Kidney Int* 1994; 46: 965–972
9. Van Der Helm-Van Mil AH, Smith AC, Pouria S *et al.* Immunoglobulin A multiple myeloma presenting with Henoch-Schonlein purpura associated with reduced sialylation of IgA1. *Br J Haematol* 2003; 122: 915–917
10. Zickerman AM, Allen AC, Talwar V *et al.* IgA myeloma presenting as Henoch-Schonlein purpura with nephritis. *Am J Kidney Dis* 2000; 36: E19
11. Dosa S, Cairns SA, Mallick NP *et al.* Relapsing Henoch-Schonlein syndrome with renal involvement in a patient with an IgA monoclonal gammopathy. A study of the results of immunosuppressant and cytotoxic therapy. *Nephron* 1980; 26: 145–148
12. Terness P, Navolan D, Moroder L *et al.* A natural IgA-anti-F(ab') 2gamma autoantibody occurring in healthy individuals and kidney graft recipients recognizes an IgG1 hinge region epitope. *J Immunol* 1996; 157: 4251–4257
13. Nishie T, Miyaishi O, Azuma H *et al.* Development of immunoglobulin A nephropathy-like disease in beta-1,4-galactosyltransferase-I-deficient mice. *Am J Pathol* 2007; 170: 447–456
14. Amore A, Cirina P, Conti G *et al.* Glycosylation of circulating IgA in patients with IgA nephropathy modulates proliferation and apoptosis of mesangial cells. *J Am Soc Nephrol* 2001; 12: 1862–1871
15. Chen N, Nusbaum P, Halbwachs-Mecarelli L *et al.* Light-chain composition of serum IgA1 and in vitro IgA1 production in IgA nephropathy. *Nephrol Dial Transplant* 1991; 6: 846–850
16. Monteiro RC, Halbwachs-Mecarelli L, Roque-Barreira MC *et al.* Charge and size of mesangial IgA in IgA nephropathy. *Kidney Int* 1985; 28: 666–671
17. Lai KN, To WY, Li PK *et al.* Increased binding of polymeric lambda-IgA to cultured human mesangial cells in IgA nephropathy. *Kidney Int* 1996; 49: 839–845

18. Coppo R, Amore A, Roccatello D. Dietary antigens and primary immunoglobulin A nephropathy. *J Am Soc Nephrol* 1992; 2: S173–S180
19. Sategna-Guidetti C, Ferfoglia G, Bruno M *et al.* Do IgA antigliadin and IgA antiendomysium antibodies show there is latent coeliac disease in primary IgA nephropathy? *Gut* 1992; 33: 476–478
20. Monteiro RC, Chevailler A, Noel LH *et al.* Serum IgA preferentially binds to cationic polypeptides in IgA nephropathy. *Clin Exp Immunol* 1988; 73: 300–306

Received for publication: 29.7.10; Accepted in revised form: 16.2.11